Aerosol and Air Quality Research, 14: 1998–2009, 2014

ISSN: 1680-8584 print / 2071-1409 online
doi: 10.4209/aaqr.2014.09.0201

Influences of Beehive Firework Displays on Ambient Fine Particles during the Lantern Festival in the YanShuei Area of Southern Taiwan

Chih-Chung Lin[1], Kuo-Lin Huang[1], Hsiu-Lin Chen[2], Jen-Hsiung Tsai[1], Yu-Ping Chiu[1], Jia-Twu Lee[1], Shui-Jen Chen[1*]

[1] *Department of Environmental Science and Engineering, National Pingtung University of Science and Technology, Nei-Pu, Pingtung, Taiwan*
[2] *Department of Industrial Safety and Health, Hung Kuang University, Taichung, Taiwan*

ABSTRACT

This study investigates water-soluble ions in the sized particles (particularly Aitken nuclei mode (dp ≤ 0.1 µm, $PM_{0.1}$)/ accumulation mode (0.1 < dp ≤ 1.0 µm, $PM_{0.1-1.0}$)) collected using a MOUDI sampler in the YanShuei area of southern Taiwan during a beehive fireworks display. The results indicate that the $PM_{2.5}$ and PM_{10} concentrations (437 µg/m^3 and 572 µg/m^3, respectively) at the leeward sampling site are 12.5 and 4.6 times higher than the corresponding national standards of daily mean values (35 and 125 µg/m^3, respectively) during the beehive fireworks display. Closely examining PM accumulation fractions reveals that the accumulation mode particles dominate in the sized collected particles during the beehive fireworks display. Additionally, the K^+ concentrations in $PM_{1.0}$, $PM_{2.5}$, and $PM_{2.5-10}$ are 317, 349, and 249 times higher than those of its background value, while those of Cl^- are 91, 64, and 6.9 times greater than those of its background value. For ultrafine particles, the D/B (During the beehive fireworks display/Background) values of particle-bound Cl^-, K^+, and Mg^{2+} increase significantly during the beehive fireworks display at the leeward sampling site. Moreover, the maxima D/B value of K^+ is 196 in the 0.1–0.18 µm size range, revealing that the beehive firework aerosols are rich in Cl^-, K^+, and Mg^{2+} ions.

Keywords: Beehive fireworks display; Ultrafine; Water-soluble ions; Short-term pollution.

INTRODUCTION

Short-term or instantaneous air pollution effects on health have received increasing attention in recent years, as evidenced by numerous efforts to characterize anthropogenic emissions, especially in urban areas where large populations live (Ravindra *et al.*, 2003; Kulshrestha *et al.*, 2004; Chang *et al.*, 2013; You *et al.*, 2013). The extensive use of pyrotechnics in large celebration events often significantly degrades short-term air quality, possibly harming human health (Smith and Dinh, 1975; Clark, 1997; Gorbunov *et al.*, 2013). An unusual source of atmospheric pollution) is the displacement of fireworks to celebrate festivities worldwide.

As is well known, ambient fine particle concentrations increase with fireworks displays (Vecchi *et al.*, 2008). Fireworks burning may raise levels of particulate matters (Vecchi *et al.*, 2008) containing water-soluble ions, metallic elements, and organic compounds (Liu *et al.*, 1997; Ravindra *et al.*, 2003; Kulshrestha *et al.*, 2004; Drewnick *et al.*, 2006; Moreno *et al.*, 2007; Wang *et al.*, 2007; Steinhauser *et al.*, 2008). Zhang *et al.* (2010) found that particle concentrations during the peak hour of firework celebrations are approximately three times higher than the day before celebration, with a clear shift of particles from nuclei mode (10–20 nm) and Aitken mode (20–100 nm) to accumulation mode (0.5–1.0 µm). According to these studies (Wang *et al.*, 2007; Chang *et al.*, 2011; Huang *et al.*, 2012; Tsai *et al.*, 2012b), extensive burning of fireworks causes significant increases in the levels of $PM_{2.5}$ and PM_{10} bound elements and water-soluble ions, as well as in the number concentration of particles in the size range of 100–500 nm.

Many studies have noted elevated concentrations of water-soluble ions (K^+, Cl^-, and SO_4^{2-}) in ambient aerosol particles during and shortly after fireworks displays (Ravindra *et al.*, 2003; Drewnick *et al.*, 2006; Moreno *et al.*, 2007; Wang *et al.*, 2007; Shen *et al.*, 2009; Godri *et al.*, 2010; Tsai *et al.*, 2012a; Satsangi *et al.*, 2013; You *et al.*, 2013; Yang *et al.*, 2014). However, the mass concentrations and chemical compositions (water-soluble ions components/ concentrations) of $PM_{0.1}$, $PM_{1.0}$, $PM_{2.5}$, and $PM_{2.5-10}$ from beehive fireworks displays have seldom been studied. Therefore, this study investigates the mass concentrations

* Corresponding author.
Tel.: +886-8-7740263; Fax: +886-8-7740256
E-mail address: chensj@mail.npust.edu.tw

in $PM_{0.1}$, $PM_{1.0}$, $PM_{2.5}$ and $PM_{2.5–10}$, as well as determines the water-soluble ion components (Na^+, K^+, NH_4^+, Mg^{2+}, Ca^{2+}, Cl^-, NO_3^-, and SO_4^{2-})/concentrations in sized particles collected in the YanShuei area of southern Taiwan. The size distributions and cumulative mass fractions of particles/water-soluble ions for each particle size range are based on the samples of particles collected by a MOUDI sampler. Analysis results demonstrate that a beehive fireworks display emits a significant amount of ultrafine particles instantaneously and degrades short-term air quality, thereby necessitating attention to address health concerns.

MATERIALS AND METHODS

Collection of Particulates

Atmospheric particulate samples were collected in the YanShuei area of southern Taiwan during the Lantern Festival from February 21 to 25 in 2013. The windward sampling site was located on the roof of a three-story building (9 m height) in the Wumiao Temple, roughly 50 m north to the major beehive fireworks display site, while the leeward sampling site was located on the roof of a four-story building (12 m height) in the YanShuei police office, roughly 300 m south to the major beehive fireworks display site. The YanShuei beehive fireworks display events occurred within the four stages of our experimental periods. In this investigation, it is regarded that February 21th–22th, 23th–24th, 24th (18:00–24:00), and 25th 2013 were the before (background), trial, during, and after beehive fireworks display periods, respectively. The mean air temperature, relative humidity, and wind speed were 19.1 (14.4–26.4)°C, 78.9 (56.0–94.0)%, and 0.54 (0.0–2.2) m/s, respectively, during the sampling period (without any rain).

A MOUDI (Model No.100; MSP Co., Minneapolis, MN) sampler equipped with Teflon filters (with diameters of 37 mm) was used to collect size-resolved aerosol samples. These impactors effectively separated the particulate matter into 10 ranges (at 50% efficiency) with the following equivalent cut-off diameters; 18–10, 10–5.6, 5.6–3.2, 3.2–1.8, 1.8–1.0, 1.0–0.56, 0.56–0.32, 0.32–0.18, 0.18–0.1, and 0.1–0.056 µm. Accordingly, the particles were divided into four size groups - coarse ($PM_{2.5–10}$), fine ($PM_{2.5}$), accumulation ($PM_{0.01–1.0}$: 0.01 µm < D_p ≤ 1.0 µm), and ultrafine ($PM_{0.01–0.1}$: 0.01 µm < D_p ≤ 0.1 µm) particles. The sampling flow rate for the MOUDI was 30 L/min.

Silicon grease was applied to the surface of each filter installed in the MOUDI sampler, and the greased filter-strips were baked in a 60°C oven for 90 min to stabilize the silicon grease before sampling to minimize particle bounce between the different stages of the MOUDI during the sampling. Before and after each sampling, the filters were dried for 24 h in a desiccator at 25°C in 40% relative humidity. They were then weighed on an electronic balance (AND HM202) with a resolution of 10 µg. The suspended particulate matter concentration was determined by dividing the particle mass by the volume of sampled air.

Water-Soluble Ion Analysis and Quality Control

Before the property of the particle-bound water-soluble inorganic species (Na^+, K^+, NH_4^+, Mg^{2+}, Ca^{2+}, Cl^-, NO_3^-, and SO_4^{2-}) were determined quantitatively, collected particles from each Teflon fiber filter had been extracted using 10 mL of ultra-pure water (specific resistance 18.3 MΩcm). The water-soluble ions were extracted using an ultrasonic bath (UC-300) for 120 minutes. All extraction solutions were filtered through a cellulose acetate filter (ADVANTEC MFS, Inc., USA cat No., CO20A025A; pore size of 0.2 µm; diameter of 25 mm) and stored in plastic vials in a refrigerator at 4°C until they were chemically analyzed. The inorganic species were analyzed by ion chromatography (IC) (DIONEX ICS-3000 with conductivity detection (DC detector/chromatography module, P/N 061767)). The cations were identified using a DIONEX IonPac® 4 × 50 mm CG12A guard column, a DIONEX IonPac® 4 × 250 mm CS12A analytical column, and a cation self-regenerating suppressor (CSRS® ULTRA II, 4 mm, AutoSuppression® Recycle Mode); the anions were identified using a DIONEX IonPac® 4 × 50 mm AG11 guard column, a DIONEX IonPac® 4 × 250 mm AS11 analytical column, and an anion self-regenerating suppressor (ASRS® ULTRA II, 4 mm, AutoSuppression® Recycle Mode). The eluents for the cation and anion analyses were 20 mM of methane sulfonic acid and 12 mM of NaOH, respectively. Analytical drift was monitored throughout the analytical procedures. Next, recovery efficiencies were determined using diluted samples that were spiked with known quantities of the ions of interest. Recovery efficiencies ranged from 93% to 107%. The method detection limit (MDL) was estimated by repeatedly analyzing a control solution of known quality. Replicate analysis of IC measurements was performed to calculate the MDL of each element using MDL = 2.681 × S_{pooled}, with $S_A^2/S_B^2 < 3.05$. $S_{pooled} = [(6S_A^2 + 6S_B^2)/12]^{0.5}$, where S_{pooled} denotes the pooled standard deviation; S_A represents the standard deviation of property of the prepared sample with a larger F-test value, and S_B is the standard deviation of the other sample. The detection limits in ng/m^3 (estimated from MDL × volume of analyte solution (10 mL)/average sampling volume (20 m^3)) were Na^+, 7.00 ng/m^3; K^+, 12.0 ng/m^3; NH_4^+, 27.0 ng/m^3; Mg^{2+}, 13.0 ng/m^3; Ca^{2+}, 10.5 ng/m^3; Cl^-, 46.6 ng/m^3; NO_3^-, 28.6 ng/m^3; and SO_4^{2-}, 61.6 ng/m^3. Both field and laboratory blank samples were prepared and analyzed for each sampling and analysis. All data were corrected with blanks.

RESULTS AND DISCUSSION

Atmospheric Particle Concentrations and Mass Size Distributions

Table 1 lists the concentrations of particles before (background), trial, during, and after a beehive fireworks display in the 2013 YanShuei Fireworks Festival on the rooftop of the Wumiao Temple (windward) and YanShuei police office (leeward). At the windward sampling site, the $PM_{0.1}$, $PM_{1.0}$, $PM_{2.5}$, and $PM_{2.5–10}$ concentrations were 0.767, 17.4, 26.1, and 19.3 µg/m^3, respectively, before beehive fireworks display (background). Corresponding data were 2.48, 30.6, 46.1, and 39.3 µg/m^3, respectively, at the trial stage (approximately 120 thousand fireworks rockets) and

Table 1. PM concentrations and $PM_{2.5}/PM_{10}$ values at the four periods (before (background), trial, during, and after) of a beehive fireworks display.

Sampling site	Sampling periods	PM (μg/m^3)				$PM_{2.5}/PM_{10}$
		$PM_{0.1}$	$PM_{1.0}$	$PM_{2.5}$	$PM_{2.5–10}$	
Windward	Background	0.767	17.4	26.1	19.3	0.57
	Trial	2.48	30.6	46.1	39.3	0.54
	During	11.3	120	165	57.0	0.74
	After	1.36	45.7	103	45.0	0.70
Leeward	Background	1.73	20.9	28.2	12.4	0.69
	Trial	9.86	77.9	120	61.0	0.66
	During	2.73	321	437	135	0.76
	After	1.67	43.5	107	56.0	0.66

11.3, 120, 165, and 57.0 μg/m^3, respectively, during the beehive fireworks display (> 10 million fireworks rockets). After the display, the values were 1.36, 45.7, 103, and 45.0 μg/m^3, respectively. On the other site (leeward), the $PM_{0.1}$/$PM_{1.0}$/$PM_{2.5}$/$PM_{2.5–10}$ concentrations were 1.73/20.9/28.2/12.4, 9.86/77.9/120/61.0, 2.73/321/437/135, and 1.36/45.7/103/45.0 μg/m^3, at the before, trial, during, and after the beehive fireworks display, respectively. $PM_{2.5}$ concentrations greater than 437 μg/m^3 during the beehive fireworks may cause adversely impact the health of susceptible individuals. However, these adverse effects are limited, owing to the short exposure to the peak concentrations. Yang *et al.* (2014) found higher $PM_{2.5}$ concentrations (maximum = 464.02 μg/m^3) during the 2008 Chinese New Year period than in previous years. High $PM_{2.5}$ concentrations were also observed (range = 117–217 μg/m^3; average = 183 μg/m^3, i.e. roughly six times higher than those before and after the Chinese New Year) in the Yellow River Delta region during the Chinese New Year in 2011 (Li *et al.*, 2013).

Before the YanShui beehive fireworks display, the $PM_{2.5}$ concentrations were 26.1 and 28.2 μg/m^3, respectively, at the windward and leeward sampling sites, while the PM_{10} ones were 45.4 and 40.6 μg/m^3, respectively. Notably, the $PM_{2.5}$ and PM_{10} concentrations of air quality standards in Taiwan are 35 and 125 μg/m^3, respectively. At the windward and leeward sampling sites, the $PM_{2.5}/PM_{10}$ ratios were 0.57 and 0.69, respectively. Moreover, the $PM_{2.5}$ concentration significantly increased during the YanShui beehive fireworks display, and the $PM_{2.5}/PM_{10}$ ratios) obviously increased to 0.74 and 0.76 at the windward and leeward, respectively. Tsai *et al.* (2012b) indicated that the $PM_{2.5}/PM_{10}$ ratios observed during the fireworks display periods ranged from 0.61 to 0.73 with an average of 0.69. In the center of Mainz, a small city in central Germany (population 120,000), the average total mass concentration measured by a time-of-flight aerosol mass spectrometer (TOF-AMS) for the entire day of January 1 was 51.0 μg/m^3 (Drewnick *et al.*, 2006). Shen *et al.* (2009) sampled $PM_{2.5}$ for 24 hours in XiAn using Dichot samplers during the fireworks display during the Chinese New Year. According to their results, the average $PM_{2.5}$ concentration was 300 μg/m^3, i.e., 3–4 times higher than the regular value obtained when no fireworks were displayed.

At the leeward site, the $PM_{0.1}$ concentration after the fireworks display was 1.67 μg/m^3, i.e., lower than the background value (1.73 μg/m^3). Whereas the value was 9.86 μg/m^3 during the trial stage, i.e., higher than that (2.73 μg/m^3) during the beehive fireworks display. During the 4 periods of the beehive fireworks display, the $PM_{1.0}$, $PM_{2.5}$, and $PM_{2.5–10}$ concentrations were the highest during the beehive fireworks display and the lowest before the beehive fireworks display (background values). During the four periods (before (background), trial, during, and after) of the beehive fireworks display, the concentrations of sized PMs were lower at the windward site than those at the leeward one, except that of $PM_{0.1}$ during beehive fireworks display and that of background $PM_{2.5–10}$. This finding suggests that festival attendees on the leeward of beehive fireworks displaying area had a greater risk of high concentration PM exposure than those at the windward site.

Particle Mass Size Distributions and Accumulation Fractions

Particle mass size distributions at YanShui before (background), trial, during, and after the beehive fireworks display were all bi-modal distribution with one main peak in the fine size range and the other in the coarse size domain (Figs. 1–3). At both of the windward and leeward sampling sites, the major peaks of particle mass size distributions were in the accumulation mode (0.56–1.0 μm) during the beehive fireworks display; however, they were in the drop mode (1.0–1.8 μm) after the display. Yang *et al.* (2014) indicated that the widespread burning of fireworks during the 2008 Chinese New Year obviously contributed to the number concentration of small accumulation mode particles (100–500 nm).

At the windward sampling site, the background accumulation fractions of $PM_{0.1}$, PM_1, and $PM_{2.5}$ were 4.1, 47.7, and 64.3%, respectively; 5.2, 41.4, and 63.9%, respectively, during the trial display stage; 0.4, 52.9, and 71.8%, respectively, during the beehive fireworks display period; and 1.0, 25.2, and 62.1%, respectively, after the display (Fig. 4). At the leeward sampling site, the corresponding values were 1.6, 35.5, and 53.3%, respectively, for the background period; 2.6, 32.2, and 48.5%, respectively, during the trial display stage; 4.7, 50.3, and 68.9%, respectively, during the beehive fireworks display period; and 0.9, 29.9, and 67.6%, respectively, after the display (Fig. 5). Above results indicate that most of the particles produced during the beehive fireworks display were in the

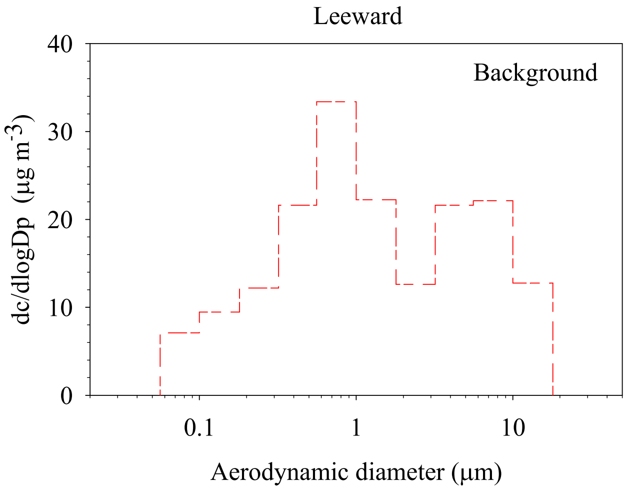

Fig. 1. Particle mass size distribution before beehive fireworks display at the leeward.

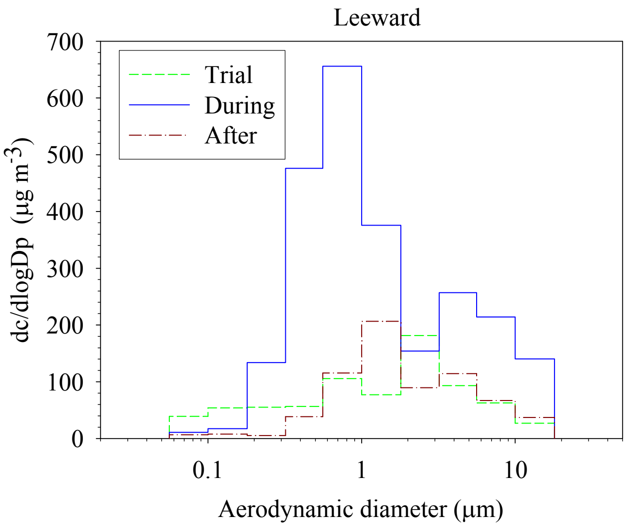

Fig. 2. Particle mass size distributions at trial, during, and after beehive fireworks display periods at the leeward.

accumulation mode. Yang *et al.* (2014) found that dominated in size fractions, Aitken and accumulation mode particles accounting for 57% and 42%, respectively, of the total particle number concentration during the 2008 Chinese New Year period.

At both sampling sites, the mean accumulation fractions of PM_1 during the beehive fireworks display period approximately increased by 10 to 18% over those during the trial display period. Meanwhile, the corresponding values during the beehive fireworks display period were approximately 2.0 times those after the display. Above results imply that the beehive fireworks display affected the size distribution of local atmospheric particles, which may be associated with the growth of Aitken-mode aerosols and their transformation into fine-mode ones by condensation, coagulation, aggregation, and aging during the transport.

Impact of Firework/Fireworks Display on Airborne Particles

Table 2 displays the concentration ratios of sized particles collected during the four sampling periods at the Wumiao temple (windward) and the YanShuei police office (leeward). During the trial fireworks display period, the $PM_{0.1}$, $PM_{1.0}$, $PM_{2.5}$, and $PM_{2.5–10}$ concentrations were 3.2, 1.8, 1.8, 2.0 times higher than the background values, respectively, at the windward sampling site; meanwhile, those at the leeward sampling site were 5.7, 3.7, 4.3, and 4.9 times greater than the background ones. During the beehive fireworks display period, the corresponding times were 14.7, 6.9, 6.3, and 3.0, respectively, at windward, and 1.6, 15.4, 15.5, and 10.9, respectively, at leeward. After the fireworks display, the $PM_{0.1}$, $PM_{1.0}$, $PM_{2.5}$, and $PM_{2.5–10}$ concentrations at windward were still (1.8, 2.6, 3.9, and 2.3 times, respectively) higher than the background data; this was also true for those of $PM_{1.0}$, $PM_{2.5}$, and $PM_{2.5–10}$ at leeward (2.1, 3.8, and 4.5 times, respectively). However, the $PM_{0.1}$ concentration (1.67 $\mu g/m^3$) was close to that of the background value (1.73 $\mu g/m^3$).

The background $PM_{2.5}$ and PM_{10} concentrations at windward were 26.1 and 45.4 $\mu g/m^3$, respectively, and those

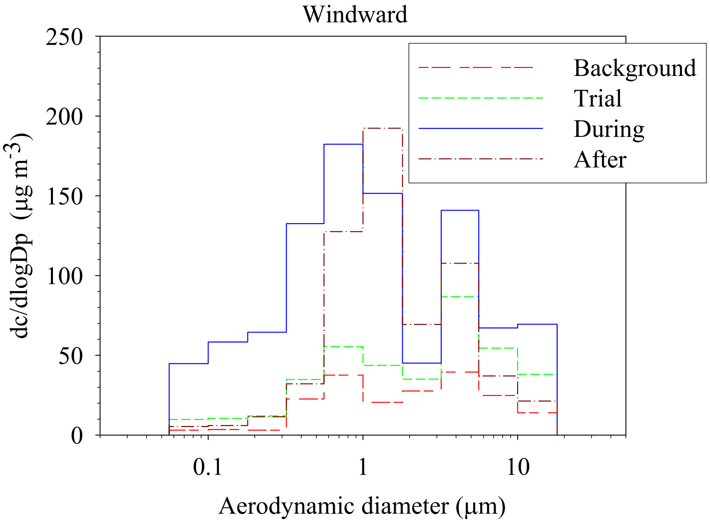

Fig. 3. Particle mass size distributions of before (background), trial, during, and after beehive fireworks display periods at the windward.

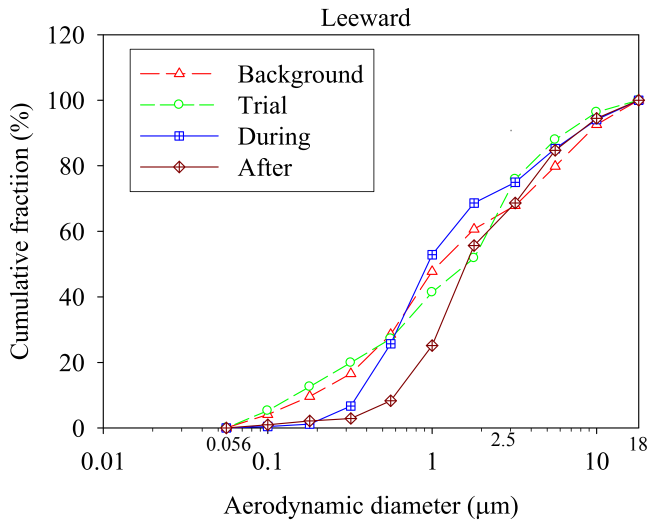

Fig. 4. Cumulative mass fractions of the particles collected of before (background), trial, during, and after beehive fireworks display periods at the leeward.

at leeward were lower (28.2 and 40.6 µg/m^3, respectively), thereby complying with the national air quality standards (35 and 125 µg/m^3, respectively). During the beehive fireworks display, the $PM_{1.0}$ concentrations at the windward and leeward sampling sites were 120 and 321 µg/m^3, respectively, which were 6.9 and 15.4 times higher than the background values. Moreover, the $PM_{2.5}$ and PM_{10} concentrations also exceeded the national standards. At the windward sampling site, the $PM_{2.5}$ and PM_{10} concentrations were 165 µg/m^3 and 222 µg/m^3, respectively, i.e., approximately 4.7 and 4.9 times higher than the background values, respectively, whereas at leeward those of $PM_{2.5}$ and PM_{10} (437 µg/m^3 and 572 µg/m^3, respectively) were 12.5 and 4.6 times greater than the national standards (35 and 125 µg/m^3, respectively). According to a related study on how firecrackers and fireworks display during the 2014 Chinese New Year affect ambient fine particles, the mass concentration of $PM_{2.5}$ reached ~464 µg/m^3 during the firecracker display, i.e., around four times higher than the average value (114 µg/m^3) of the non-firecracker period (Yang *et al.*, 2014). Correspondingly, Barman *et al.* (2008) also observed that the PM_{10} concentration in Diwali was ~1206 µg/m^3, which was 4 times higher than that without fireworks display.

Effect of Firework Displays on Ambient Particles Size Distribution

According to Kulmala *et al.* (2004), atmospheric particles can be divided into three size groups: Aitken nuclei mode ($dp \leq 0.1$ µm, $PM_{0.1}$), accumulation mode ($0.1 < dp \leq 1.0$ µm, $PM_{0.1-1.0}$), and coarse mode ($dp > 1.0$ µm: $1.0 < dp \leq 2.5$ µm and $2.5 < dp \leq 10$ µm two size ranges). Table 3 shows the accumulation fractions of particles in these size ranges. About half of the PM_{10} concentrations were in the Aitken nuclei ($PM_{0.1}$) and Accumulation ($PM_{0.1-1.0}$) modes

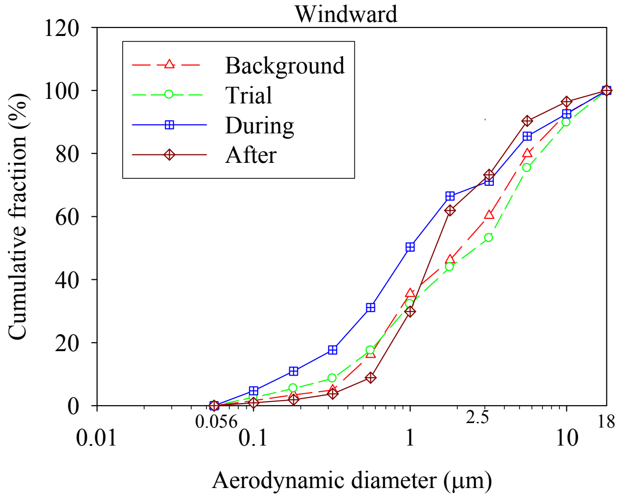

Fig. 5. Cumulative mass fractions of the particles collected of before (background), trial, during, and after beehive fireworks display periods at the windward.

Table 2. T/B, D/B, and A/B values of before (background (B)), trail (T), during (D), and after (A) beehive fireworks display periods.

Sampling site	$PM_{0.1}$			$PM_{1.0}$			$PM_{2.5}$			$PM_{2.5–10}$		
	T/B	D/B	A/B	T/B	D/B	A/B	T/B	D/B	A/B	T/B	D/B	A/B
Windward	3.2	14.7	1.8	1.8	6.9	2.6	1.8	6.3	3.9	2.0	3.0	2.3
Leeward	5.7	1.6	0.96	3.7	15.4	2.1	4.3	15.5	3.8	4.9	10.9	4.5

Table 3. Accumulation fractions (%) of PMs with dp sizes in different modes (Aitken nuclei, accumulation, and coarse modes).

Sampling site	Period	Accumulation fractions (%)			
		Aitken	Accumulation	Coarse	
		dp ≤ 0.1 μm	0.1 < dp ≤ 1.0 μm	1.0 < dp ≤ 2.5 μm	2.5 < dp ≤ 10 μm
Windward	Background	1.7	36.6	19.2	43.0
	Fireworks display	5.1	49.0	20.3	26.0
Leeward	Background	4.3	47.2	18.0	31.0
	Fireworks display	0.42	55.6	20.3	24.0

before beehive fireworks display at leeward. At the windward site, the accumulation fraction of $PM_{1.0}$ was 38.3% (1.7% + 36.6%); it was 51.5% (4.3% + 47.2%) at leeward. The accumulation fractions of coarse mode PMs (dp >1.0 μm) were 62.2% (19.2% + 43.0%) and 49% (18% + 31%) at the windward and leeward sites, respectively. During the fireworks display, the Accumulation mode PM (submicron particles easily entering the human respiratory system (alveolar region)) increased the most in accumulation fraction percentage among the three mode PMs. The percentage of PM_{10} in Accumulation mode increased by ~12% (= 49% – 36.6%) at the windward site; the increase was ~9% (= 55.6% – 47.2%).

Contrast between Concentrations of Particles with Various Diameters at the Two Sampling Sites

At the leeward sampling site, the $PM_{0.1}/PM_{2.5}$ values resembled each other before and after beehive fireworks display (Fig. 6); those at both sampling sites (0.73 and 0.74, respectively) also resembled each other (Figs. 6 and 7). Also, the $PM_{0.1}/PM_{2.5}$ value during the beehive fireworks display was higher than those of trial and after display periods, probably due to the significant increase of accumulation mode of $PM_{2.5}$. The lower ratios (0.44 and 0.41 at leeward and windward, respectively) after beehive fireworks display originated from the larger increase of $PM_{1.0–2.5}$ in $PM_{2.5}$, as shown in Table 1. The ratios of $PM_{0.1}/PM_{2.5}$ (ultrafine to fine particles) before and after the display at the four sampling periods at both sites ranged from 0.01 to 0.08 (average = 0.04). Similar individual $PM_{0.1}/PM_{2.5}$ ranges (and averages) were obtained at both sites. However, the increase (by 6.25%) of ultrafine particle concentration in $PM_{2.5}$ at the windward site during beehive fireworks display should be of concern in terms of its adverse effect on human health.

Concentrations of Particulate Water-Soluble Ions with Various Particle Diameters before and after the Display

Tables 4 and 5 present the concentrations of water-soluble ions (Na^+, K^+, Mg^{2+}, Ca^{2+}, NH_4^+, Cl^-, NO_3^-, and SO_4^{2-}) in

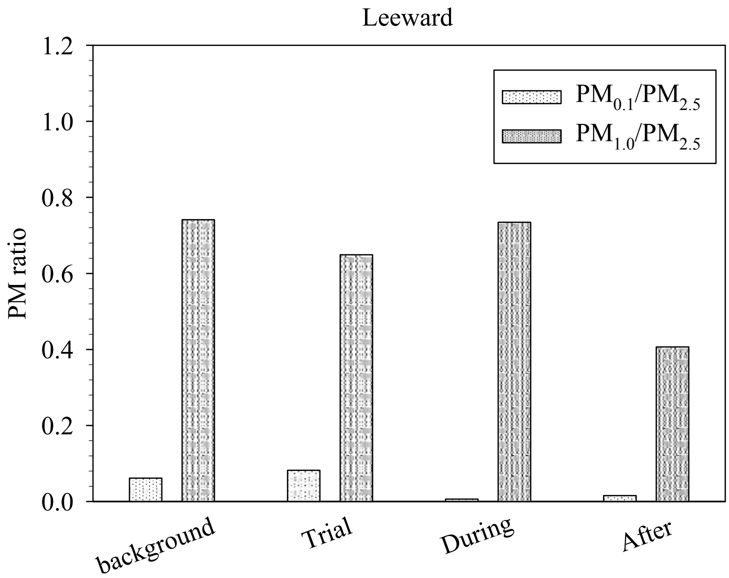

Fig. 6. Ratios of $PM_{0.1}/PM_{2.5}$ and $PM_{1.0}/PM_{2.5}$ of four sampling periods at the leeward site.

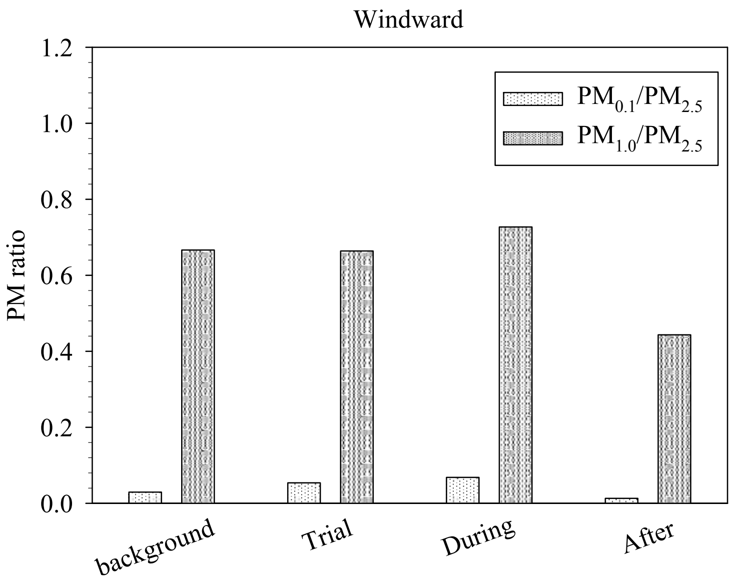

Fig. 7. Ratios of $PM_{0.1}/PM_{2.5}$ and $PM_{1.0}/PM_{2.5}$ of four sampling periods at the windward site.

$PM_{1.0}$, $PM_{2.5}$, and $PM_{2.5–10}$ at the windward and leeward sampling sites, respectively. These tables reveal that, except for Ca^{2+} in $PM_{1.0}$ at the leeward site, the concentrations of the other eight ions in $PM_{1.0}$ and $PM_{2.5}$ sampled at both sites during the fireworks display were higher than the background value. Among the tested ions, K^+ exhibited the highest increase in concentration owing to the fireworks display; the concentrations of K^+ in both $PM_{1.0}$ and $PM_{2.5}$ at the leeward site were 317 and 349 times higher than those of background values, respectively. Mg^{2+} had the second (112 and 66 times higher, respectively) and Cl^- showed the third (91 and 64 times higher, respectively) highest increase in concentration. The significant increases of these three ions in PM are likely owing to the KNO_3, $KClO_4$, $KClO_3$, $K_2Cr_2O_4$, and $K_2Cr_2O_7$ (used as oxidants) in fireworks.

During and after the fireworks display, the concentrations of the eight ions in $PM_{2.5–10}$ at the leeward site were also higher than their corresponding background values. In particular, during the beehive fireworks display, the concentration of K^+ in $PM_{2.5–10}$ was 7.22 μg/m^3, approximately 249 times than its background value (0.029 μg/m^3). The fireworks are composed mainly of KNO_3, $KClO_4$, $KClO_3$, $K_2Cr_2O_4$, $K_2Cr_2O_7$, carbon dust, and sulfur. When the fireworks were ignited, potassium nitrate was catalyzed and then helped to produce CO_2, leading to increases in the instantaneous pressure and pushes of firework rockets in the air and, finally, their explosion. After the explosion, the ashes contained not only NO_3^- and SO_4^{2-}, but also K^+ and Cl^-, which were detected at the leeward sampling site. According to our results, the

Table 4. Concentrations of water-soluble ions in $PM_{1.0}$, $PM_{2.5}$, and $PM_{2.5–10}$ at the windward sampling site.

Particle size	Sampling period	PM (μg/m³)	Water-soluble ions concentration (μg/m³)							
			Na^+	K^+	Mg^{2+}	Ca^{2+}	NH_4^+	Cl^-	NO_3^-	SO_4^{2-}
$PM_{1.0}$	Background	17.4	0.660	0.597	0.0275	0.204	1.36	0.232	2.69	1.61
	Trial	30.6	0.675	0.160	0.136	0.313	3.19	0.315	7.13	3.90
	During	120	1.73	1.95	0.145	0.316	9.30	1.64	32.4	4.58
	After	45.7	3.19	0.216	0.0502	0.452	4.23	0.914	8.65	5.34
$PM_{2.5}$	Background	26.1	1.37	0.751	0.0536	0.326	1.98	0.435	3.99	2.38
	Trial	46.1	0.917	0.213	0.167	0.403	4.03	0.413	9.28	4.85
	During	165	1.96	2.33	0.187	0.348	13.4	2.21	45.3	6.60
	After	103	5.36	0.425	0.0945	0.523	9.44	1.66	18.6	14.0
$PM_{2.5–10}$	Background	19.3	2.07	0.216	0.109	0.244	0.914	1.31	2.89	0.723
	Trial	39.3	1.90	0.110	0.240	0.376	1.73	2.39	7.32	0.762
	During	57.0	0.845	0.359	0.112	0.177	4.16	0.935	16.6	0.664
	After	45.0	3.85	0.162	0.203	0.401	2.41	1.07	8.24	2.20

Table 5. Concentrations of water-soluble ions in $PM_{1.0}$, $PM_{2.5}$, and $PM_{2.5–10}$ of four sampling periods at the leeward sampling site.

Particle size	Sampling period	PM (μg/m³)	Water-soluble ions concentration (μg/m³)							
			Na^+	K^+	Mg^{2+}	Ca^{2+}	NH_4^+	Cl^-	NO_3^-	SO_4^{2-}
$PM_{1.0}$	Background	20.9	0.225	0.121	0.0223	0.459	1.92	0.207	6.11	1.19
	Trial	77.9	0.224	0.0816	0.0316	0.212	2.26	0.231	7.76	0.395
	During	321	8.66	38.4	2.49	0.445	9.94	18.8	38.1	34.9
	After	43.5	1.20	0.391	0.040	0.244	5.69	0.160	9.19	5.49
$PM_{2.5}$	Background	28.2	0.519	0.127	0.0450	0.501	2.67	0.332	7.76	1.79
	Trial	120	0.256	0.105	0.0381	0.278	3.01	0.282	10.2	0.589
	During	437	13.1	44.3	2.98	0.761	17.3	21.2	59.5	40.4
	After	107	2.45	0.883	0.322	0.739	11.3	0.890	17.1	16.0
$PM_{2.5–10}$	Background	12.4	0.453	0.029	0.038	0.038	0.946	0.421	3.45	0.333
	Trial	61.0	0.199	0.014	0.027	0.0301	1.25	0.240	4.34	0.113
	During	135	9.06	7.22	0.773	1.56	6.16	2.91	20.7	6.45
	After	56.0	0.921	0.333	0.590	0.801	2.94	3.59	11.1	3.40

concentrations of K^+ and Cl^- in $PM_{1.0}$, $PM_{2.5}$, and $PM_{2.5–10}$ significantly increased, which were markedly higher than their background values during the intensive display of beehive fireworks. The concentrations of K^+ in $PM_{1.0}$, $PM_{2.5}$, and $PM_{2.5–10}$ were 317, 349, and 249 times higher than their background values; meanwhile, those of Cl^- were 91, 64, and 6.9 times greater than their background values. Large amounts of K-rich particles observed in this study are consistent with those found in some previous investigations in urban areas during firework periods (Drewnick *et al.*, 2006; Moreno *et al.*, 2007; Wang *et al.*, 2007; Joly *et al.*, 2010). Wilkin *et al.* (2007) and Shi *et al.* (2011) found a high perchlorate content in the particles in urban cites after firecracker/firework activity. Kulshrestha *et al.* (2004) also found that K increased the most in concentration in PM (i.e., 25 times higher than those of regular days) during the display of firecrackers and fireworks in Diwali in India.

Variation in the Concentrations of Water-Soluble Ions in PM with Various Diameters before and after the Display

At the windward side, the masses of secondary aerosol (including NH_4^+, NO_3^-, and SO_4^{2-} in $PM_{1.0}$, $PM_{2.5}$, and $PM_{2.5–10}$) were the lowest at four sampling periods before and after the beehive fireworks display (Tables 4 and 5). The contents of secondary aerosol in $PM_{2.5}$ and $PM_{2.5–10}$ increased with the total amount of displayed beehive fireworks. Conversely, at the leeward site, the contents of secondary aerosol in $PM_{1.0}$, $PM_{2.5}$, and $PM_{2.5–10}$ were higher than their background values. Although secondary aerosols (NH_4^+, NO_3^-, and SO_4^{2-}) were produced as fireworks displayed, incomplete combustion of fireworks (e.g., present as OC and EC) might occur in a fireworks explosion. The significant amount of incomplete combustion products from the explosion could markedly increase the carbon content in the sized PMs, resulting in their higher concentrations (compared with background values) in secondary aerosol in PMs (Tables 4 and 5). However, the amounts of secondary aerosols in PMs were lower than background ones.

At the windward sampling site, during the beehive fireworks display, the concentrations of K^+ in $PM_{1.0}$, $PM_{2.5}$, and $PM_{2.5–10}$ were 1.95, 2.33, and 0.359 μg/m³, respectively, greater than the background values (0.597, 0.751, and 0.261 μg/m³, respectively) (Table 4). The content percentages of K^+ in $PM_{1.0}$, $PM_{2.5}$, and $PM_{2.5–10}$ were 1.6, 2.33, and 0.6%, respectively. These contents were relatively lower than the background values (3.4%, 2.9%, and 1.1%, respectively). The concentrations of Cl^- in $PM_{1.0}$ and $PM_{2.5}$

during beehive fireworks display were 1.64 and 2.21 μg/m^3, respectively, which were 7.1 and 5.1 times the background values (0.232 and 0.435 μg/m^3, respectively). However, Cl^- accounts for 1.4% in $PM_{1.0}$, close to its background value (1.3%). Meanwhile, that for the value was 1.3% in $PM_{2.5}$, lower than its background value (1.7%). Additionally, the increase in measured Cl^- concentration suggests that $KClO_3$ and $KClO_4$ are used as the major oxygen sources in the firecrackers. Table 4 reveals that the concentrations of both K^+ and Cl^- in $PM_{1.0}$, $PM_{2.5}$, and $PM_{2.5-10}$ at the windward side are higher than the background ones. In contrast to the results obtained at the windward sampling site, the amounts of K^+ and Cl^- in $PM_{1.0}$, $PM_{2.5}$, and $PM_{2.5-10}$ at the leeward sampling site were the highest (17.8%, 14.9%, and 7.5%, respectively) during the intensive beehive fireworks display; they were 11, 9.3, and 2.1 times higher than their background values (1.6%, 1.6%, and 3.6%).

Obviously, the concentrations of Mg^{2+} in $PM_{2.5}$ and $PM_{2.5-10}$ increase at the leeward sampling site (Table 6). The Mg^{2+} concentrations in $PM_{2.5}$ sampled during and after the display were 2.98 and 0.322 μg/m^3, respectively; they were 66 and 7.2 times higher than the background value (0.045 μg/m^3), respectively; those in $PM_{2.5-10}$ were 0.773 and 0.590 μg/m^3, respectively, 20 and 16 times higher the background value of 0.038 μg/m^3, respectively. This finding is associated with the fact that fireworks usually consist of various compositions, including Mg and Al compounds (for displaying white flames). Moreno *et al.* (2007) studied how the fireworks displays at festivals in Spain affect the particulate matter. According to their results, the concentrations of K, Al, and Mg range from 0.5–5.9, 0.6–2.2, and 0.1–0.5 μg/m^3, respectively. A study by Wang *et al.* (2007) on the Lantern Festival in Beijing, China demonstrated that in $PM_{2.5}$ and PM_{10}, K^+ (21 times), Mg^{2+} (11 times), and Cl^- (9 times) ranked as the third largest increase in the amount of all water-soluble ions.

Ratios (T/B, D/B, and A/B) (Ratios of Values of before (Background (B)), Trail (T), During (D), and After (A) Beehive Firework Display Periods) of Particle-Bound Water-Soluble ion Compositions for Different PMs

According to Fig. 8, the D/B values of particle-bound Cl^-, K^+, and Mg^{2+} ions significantly increased in ultrafine particle during the beehive fireworks display at the leeward sampling site. The maxima D/B value of K^+ is 196 in the 0.1–0.18 μm size range. However, the D/B values of particle-bound secondary aerosol species were nearly smaller than T/B and A/B data. (Notably, the ratios of ion compositions were from 0 to 2.) This finding suggests that the particle-bound Cl^-, K^+, and Mg^{2+} increased during the beehive fireworks display, thus demonstrating that firework aerosols are rich in Cl^-, K^+, and Mg^{2+} ions.

CONCLUSIONS

This study investigates water-soluble ions in the sized particles collected using a MOUDI sampler in the YanShuei area of southern Taiwan during a beehive fireworks display. The results indicate that $PM_{2.5}$ concentrations greater than 437 μg/m^3 during the beehive fireworks may cause adversely impact the health of susceptible individuals. Particle mass size distributions at YanShui before (background), trial, during, and after the beehive fireworks display were all bi-modal distribution with one main peak in the fine size range and the other in the coarse size domain and most of the particles produced during the beehive fireworks display were in the accumulation mode. At the windward sampling site, the $PM_{2.5}$ and PM_{10} concentrations were approximately 4.7 and 4.9 times higher than the background values, respectively, whereas at leeward those of $PM_{2.5}$ and PM_{10} were 12.5 and 4.6 times greater than the national standards (35 and 125 μg/m^3, respectively). Among the tested ions, K^+ exhibited the highest increase in concentration owing to the fireworks display; the concentrations of K^+ in both $PM_{1.0}$ and $PM_{2.5}$ at the leeward site were 317 and 349 times higher than those of background values, respectively. Mg^{2+} had the second (112 and 66 times higher, respectively) and Cl^- showed the third (91 and 64 times higher, respectively) highest increase in concentration. This finding suggests that the particle-bound Cl^-, K^+, and Mg^{2+} increased during the beehive fireworks display, thus demonstrating that firework aerosols are rich in Cl^-, K^+, and Mg^{2+} ions.

Table 6. D/B and A/B values of for $PM_{1.0}$, $PM_{2.5}$, and $PM_{2.5-10}$ during the beehive fireworks display.

Sampling site	Water soluble ions	$PM_{1.0}$		$PM_{2.5}$		$PM_{2.5-10}$	
		D/B	A/B	D/B	A/B	D/B	A/B
Windward	SO_4^{2-}	2.8	3.3	2.8	5.9	0.92	3.0
	NO_3^-	12	3.2	11	4.7	5.7	2.8
	NH_4^+	6.8	3.1	6.8	4.8	4.6	2.6
	Cl^-	7.1	3.9	5.1	3.8	0.71	0.82
	K^+	3.3	0.4	3.1	0.56	1.7	0.8
	Mg^{2+}	5.3	1.8	3.5	1.8	1.0	1.9
Leeward	SO_4^{2-}	29	4.6	22	8.9	19	10
	NO_3^-	6.2	1.5	7.7	2.2	6.0	3.2
	NH_4^+	5.2	3.0	6.5	4.2	6.5	3.1
	Cl^-	91	0.77	64	2.7	6.9	8.5
	K^+	317	3.2	349	7.0	249	11
	Mg^{2+}	112	1.8	66	7.2	20	16

B: background; D: during beehive fireworks display; A: after the display.

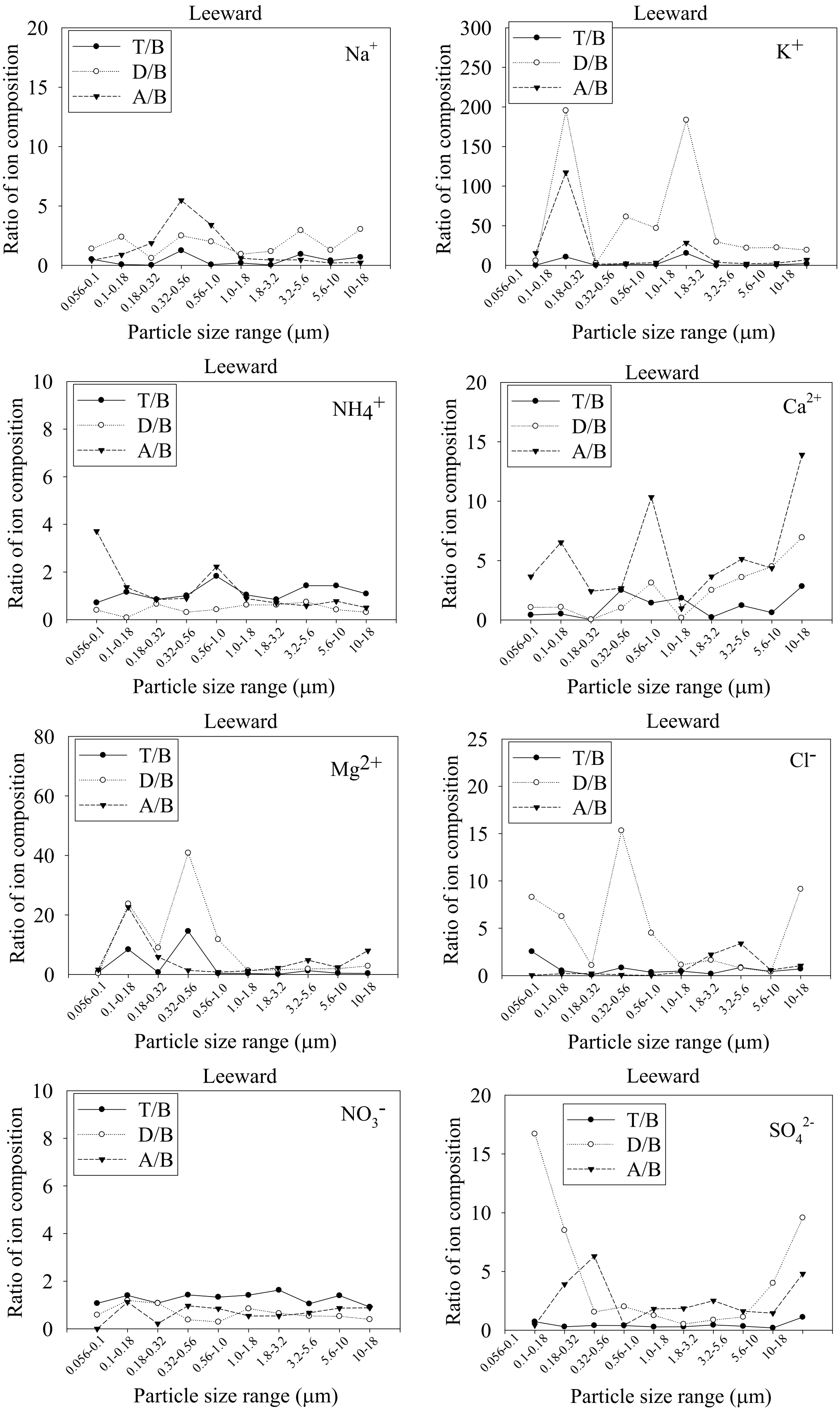

Fig. 8. T/B, D/B, and A/B values and ratios of ion compositions of particle-bound water-soluble ions in different particle size ranges at the leeward sampling sites.

REFERENCES

Barman, S.C., Singh, R., Negi, M.P.S. and Bhargava, S.K. (2008). Ambient Air Quality of Lucknow City (India) during Use of Fireworks on Diwali Festival. *Environ. Monit. Assess.* 137: 495–504.

Chang, S.C., Lin, T. H., Young, C.Y. and Lee, C.T. (2011). The Impact of Ground-Level Fireworks (13 Km Long) Display on the Air Quality during the Traditional Yanshui. *Environ. Monit. Assess.* 172: 463–479.

Chang, S.Y., Chou, C.C.K., Liu, S. and Zhang, Y. (2013). The Characteristics of $PM_{2.5}$ and Its Chemical Compositions between Different Prevailing Wind Patterns in Guangzhou. *Aerosol Air Qual. Res.* 13: 1373–1383.

Drewnick, F., Hings, S.S., Curtius, J., Eerdekens, G. and Williams, J. (2006). Measurement of Fine Particulate and Gas-Phase Species during the New Year's Fireworks 2005 in Mainz, Germany. *Atmos. Environ.* 40: 4316–4327.

Godri, K.J., Green, D.C., Fuller, G.W., Dall'osto, M., Beddows, D.C., Kelly, F.J., Harrison, R.M. and Mudway, I.S. (2010). Particulate Oxidative Burden Associated with Firework Activity. *Environ. Sci. Technol.* 44: 8295–8301.

Gorbunov, B., Muir, R., Jackson, P. and Priest, N.D. (2013). Evaluation of the Airborne Particles Fraction Responsible for Adverse Health Effects. *Aerosol Air Qual. Res.* 13: 1678–1692.

Huang, K., Zhuang, G., Lin, Y., Wang, Q., Fu, J.S., Zhang, R., Li, J., Deng, C. and Fu, Q. (2012). Impact of Anthropogenic Emission on Air Quality over a Megacity — Revealed from an Intensive Atmospheric Campaign during the Chinese Spring Festival. *Atmos. Chem. Phys.* 12: 11631–11645.

Joly, A., Smargiassi, A., Kosatsky, T., Fournier, M., Dabek-Zlotorzynska, E., Celo, V., Mathieu, D., Servranckx, R., D'amours, R., Malo, A. and Brook, J. (2010). Characterisation of Particulate Exposure during Fireworks Displays. *Atmos. Environ.* 44: 4325–4329.

Kulmala, M., Vehkamaki, H., Petajda, T., Dal Maso, M., Lauri, A., Kerminen, V-M., Birmili, W. and McMurry, P.H. (2004). Formation and Growth Rates of Ultrafine Atmospheric Particles: A Review of Observations. J. *Aerosol Sci.* 35: 143–176.

Kulshrestha, U.C., Nageswara Rao, T., Azhaguvel, S. and Kulshrestha, M.J. (2004). Emissions and Accumulation of Metals in the Atmosphere Due to Crackers and Sparkles during Diwali Festival in India. *Atmos. Environ.* 38: 4421–4425.

Li,W., Shi, Z., Yan, C., Yang, L., Dong, C. and Wang, W. (2013). Individual Metal-bearing Particles in a Regional Haze Caused by Firecracker and Firework Emissions. *Sci. Total Environ.* 443: 464–469.

Liu, D.Y., Rutherford, D., Kinsey, M. and Prather, K.A. (1997). Real Time Monitoring of Pyrotechnically Derived Aerosol Particles in the Troposphere. *Anal. Chem.* 69: 1808–1814.

Moreno, T., Querol, X., Alastuey, A., Cruz Minguillon, M., Pey, J., Rodriguez, S., Vicente Miro, J., Felis, C. and Gibbons, W. (2007). Recreational Atmospheric Pollution Episodes: Inhalable Metalliferous Particles from Firework Displays. *Atmos. Environ.* 41: 913–922.

Ravindra, K., Mor, S. and Kaushik, C.P. (2003). Short-term Variation in Air Quality associated with Firework Events: A Case Study. *J. Environ. Monit.* 5: 260–264.

Satsangi, A., Pachauri, T., Singla, V., Lakhani, A. and Kumari, K.M. (2013). Water Soluble Ionic Species in Atmospheric Aerosols: Concentrations and Sources at Agra in the Indo-Gangetic Plain (IGP). *Aerosol Air Qual. Res*. 13: 1877–138

Shen, Z., Cao, J., Arimoto, R., Han, Z., Zhang, R., Han, Y., Liu, S., Okuda, T., Nakao, S. and Tanaka, S. (2009). Ionic Composition of TSP and $PM_{2.5}$ during Dust Storms and Air Pollution Episodes at Xi'an, China. *Atmos. Environ.* 43: 2911–2918.

Shi, Y., Zhang, N., Gao, J., Li, X. and Cai, Y. (2011). Effect of Fireworks Display on Perchlorate in Air Aerosols during the Spring Festival. *Atmos. Environ.* 45: 1323–1327.

Smith, R.M. and Dinh, V.D. (1975). Changes in Forced Expiratory Flow due to Air Pollution from Fireworks. *Environ. Res.* 9: 321–331.

Steinhauser, G., Sterba, J.H., Foster, M., Grass, F. and Bichler, M. (2008). Heavy Metals from Pyrotechnics in New Years Eve Snow. *Atmos. Environ.* 42: 8616–8622.

Tsai, H.H., Chien, L.H., Yuan, C.S., Lin, Y.C., Jen, Y.H. and Ie, I.R. (2012B). Influences of Fireworks on Chemical Characteristics of Atmospheric Fine and Coarse Particles during Taiwan's Lantern Festival. *Atmos. Environ.* 62: 256–264.

Tsai, J.H., Lin, J.H., Yao, Y.C. and Chiang, H.L. (2012A). Size Distribution and Water Soluble Ions of Ambient Particulate Matter on Episode and Non-episode Days in Southern Taiwan. *Aerosol Air Qual. Res*. 12: 263–274.

Vecchi, R., Marcazzan, G. and Valli, G. (2007). A Study on Nighttime–daytime PM_{10} Concentration and Elemental Composition in Relation to Atmospheric Dispersion in the Urban Area of Milan (Italy). *Atmos. Environ.* 41: 2136–2144.

Wang, Y., Zhuang, G.S., Xu, C. and An, Z.S. (2007). The Air Pollution Caused by the Burning of Fireworks during the Lantern Festival in Beijing. *Atmos. Environ.* 41: 417–431.

Wang, Z., Wang, T., Gao, R., Xue, L.K., Guo, J., Zhou, Y., Nie, W., Wang, X., Xu, P., Gao, J. and Zhou, X. (2011). Source and Variation of Carbonaceous Aerosols at Mount Tai, North China: Results from a Semi-continuous Instrument. *Atmos. Environ.* 45: 1655–1667.

Wilkin, R.T., Fine, D.D. and Burnett, N.G. (2007). Perchlorate Behavior in a Municipal Lake following Fireworks Displays. *Environ Sci. Technol.* 41:3966–3971.

Yang, L., Gao, X., Wang, X., Nie, W., Wang, J., Gao, R., Xu, P., Shou, Y., Zhang, Q. and Wang, W. (2014). Impacts of Firecracker Burning on Aerosol Chemical Characteristics and Human Health Risk Levels during the Chinese New Year Celebration in Jinan, China. *Sci. Total Environ.* 476–477: 57–64.

You, R., Cui, W., Chen, C. and Zhao, B. (2013). Measuring the Short-Term Emission Rates of Particles in the "Personal Cloud" with Different Clothes and Activity

Intensities in a Sealed Chamber. *Aerosol Air Qual. Res*. 13: 911–921.

Zhang, M.,Wang, X.M., Chen, J.M., Cheng, T.T., Wang, T., Yang, X., Gong, Y., Geng, F. and Chen, C. (2010). Physical Characterization of Aerosol Particles during the Chinese New Year's Firework Events. *Atmos. Environ.* 44: 5191–5198.

Received for review, September 10, 2014
Accepted, October 19, 2014